



The influence of Sardinia on Corsican rainfall in the western Mediterranean Sea: A numerical sensitivity study



Florian Ehmele, Christian Barthlott*, Ulrich Corsmeier

Institute for Meteorology and Climate Research (IMK-TRO), Karlsruhe Institute of Technology (KIT), Karlsruhe, Germany

ARTICLE INFO

Article history:

Received 4 April 2014

Received in revised form 2 October 2014

Accepted 6 October 2014

Available online 22 October 2014

Keywords:

HyMeX

COSMO model

Convection initiation

Island interaction

Heavy precipitation events

ABSTRACT

The interaction of orographic effects and moisture availability is of high importance to the precipitation amount and distribution in the western Mediterranean and neighboring land surfaces. In particular, the forecast of heavy precipitation events is still a challenge for operational weather forecast models. In this study, the thermal and dynamical interactions between the two neighboring islands of Corsica and Sardinia in the western Mediterranean Sea are investigated using the Consortium for Small-scale Modeling (COSMO) model. Six cases with different synoptic conditions are analyzed and the dependence of the Corsican rainfall on the presence and terrain characteristics of Sardinia is investigated. Besides a reference run with standard model orography, sensitivity runs with removed and flat island of Sardinia are performed. The numerical results show that the daily precipitation amount over Corsica can increase by up to 220% of the amount from the reference run. Whereas most of the sensitivity runs show a decrease of the precipitation amount under strong synoptic forcing, there is no systematic relationship on days with weak synoptic forcing. The differences in the precipitation amount are induced by (i) missing deviation or missing blocking of the southerly flow by Sardinia and (ii) by the influence of cold pools generated by deep convection over Sardinia. These differences can be attributed to changes of low-level convergence and moisture/heat content and their effect on thermodynamic parameters, like convective available potential energy or convective inhibition. Furthermore, the position and translation speed of frontal systems over Corsica on days with strong synoptic forcing also depend on the Sardinian orography. These results demonstrate the high sensitivity of numerical weather prediction to the interaction of neighboring mountainous islands.

© 2014 Elsevier B.V. All rights reserved.

1. Introduction

During the late summer and autumn, most of the Mediterranean countries are regularly affected by heavy precipitation events and devastating flash floods (Llasat et al., 2010; Tarolli et al., 2012). Precipitation amounts of more than 100 mm in less than 6 h are not uncommon in these regions (Bresson et al., 2012). According to Ducrocq et al. (2008), these events are often caused by mid-latitude cyclones with embedded deep

convection or mesoscale convective systems. Despite multiple risks from hail, lightning, strong winds, and heavy precipitation, these convective systems are still an important forecasting problem in the western Mediterranean region (Fig. 1).

The highest island in this area is Corsica which features about twenty mountains being higher than 2000 m (Lambert et al., 2011). Its main mountain ridge runs from northwest to southeast with a maximum elevation of 2710 m amsl. In the framework of the Hydrological cycle in the Mediterranean Experiment (HyMeX), a multiparametric observation platform was installed in Corsica in 2012. HyMeX aims at a better understanding and quantification of the hydrological cycle and related processes in the Mediterranean with emphasis on high-impact weather events (Drobinski et al., 2014; Ducrocq et al.,

* Corresponding author at: Institute for Meteorology and Climate Research, Karlsruhe Institute of Technology (KIT), Wolfgang-Gaede-Str. 1, 76131 Karlsruhe, Germany.

E-mail address: christian.barthlott@kit.edu (C. Barthlott).

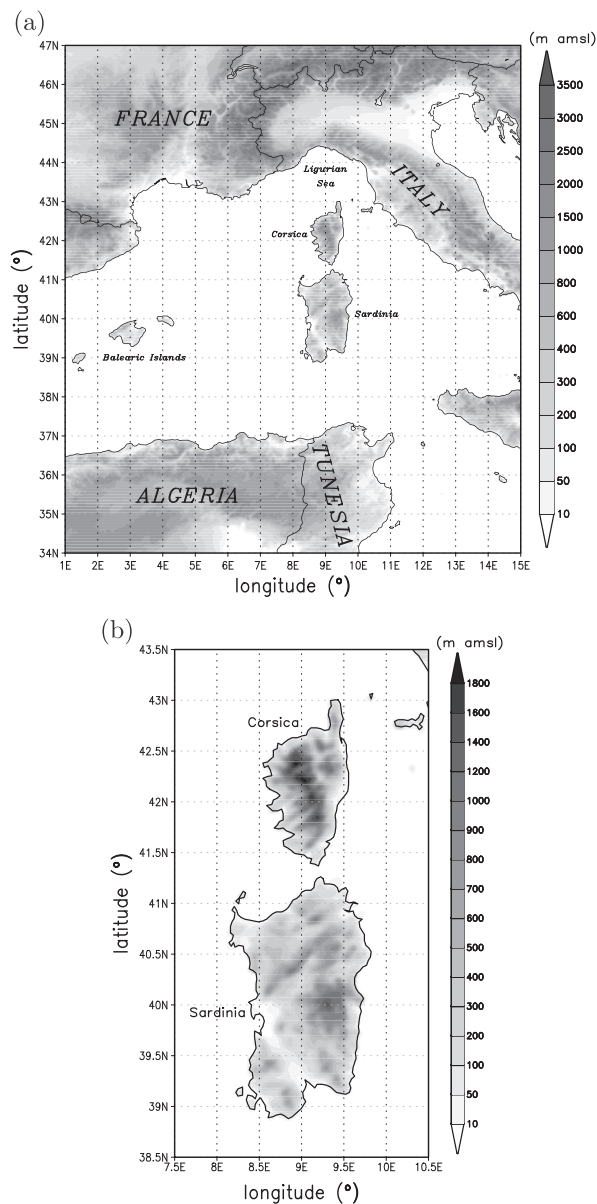


Fig. 1. The western Mediterranean Sea with the surrounding continental land masses (a) and Consortium for Small-scale MOdeling (COSMO) model topography of Corsica and Sardinia (b).

2014). As Corsica is regularly affected by intense meteorological events like heavy precipitation, lightning, or wind storms (Giorgetti et al., 1994), it is important to understand the phenomena responsible for triggering convection.

Deep convection often initiates due to mesoscale surface heterogeneities associated with variations in land use, soil moisture (e.g. Findell and Eltahir, 2003; Barthlott and Kalthoff, 2011), land–sea contrast, and orography. Mediterranean islands are hot spots for thunderstorm development due to the sharp surface heterogeneity and the low-level moisture supply by adjacent warm water bodies (e.g. Wilson et al., 2001; Qian, 2008; Robinson et al., 2008). Particularly effective at initiating convection are mountainous islands, where the sea breeze and

valley winds fall roughly into phase and the two breezes may combine to strengthen the diurnal wind cycle and form an extended sea breeze (Kottmeier et al., 2000). For the island of Corsica, Metzger et al. (2014) investigated the initiation of convection as a function of the incoming flow characteristics (instability, mid-level moisture, wind direction, and wind speed) with convection-resolving idealized numerical simulations. They found that in the case of a weak incoming flow, the location of convective triggering is determined by thermally induced circulations whereas dynamic effects prevail when the incoming flow is stronger. Furthermore, small changes in the direction of the incoming flow in the range of $\pm 30^\circ$ can discriminate between triggering and no triggering of convection. Recently, Barthlott and Kirshbaum (2013) investigated the influence of terrain forcing on the convection over Corsica and Sardinia by numerical sensitivity runs with removed and modified orography. They found that the presence of a land surface is sufficient to initiate convection, but the amount and timing of convective precipitation depend on terrain height. In addition, the proximity of Corsica to a second island of Sardinia has important effects on the low-level wind field as well as the temperature and moisture structure. Sardinia is not as high in elevation as Corsica, but roughly three times as big in horizontal extent (Fig. 1b). As the interaction between both islands may also strengthen the impact of Corsica to continental weather (Lambert et al., 2011), it is important to understand these interactions and the processes involved. By atmospheric measurements alone, those island interaction effects are difficult to assess, or not assessable at all. Therefore, we perform numerical simulations for a number of convective cases. Besides a reference run with standard model orography, we conduct sensitivity tests where we either remove the Sardinian island or where we restrict its maximum elevation to 10 m. This approach allows for identifying and separating individual processes leading to deep convection and for comparing the flow responses of two neighboring islands with different physical characteristics. In particular, we seek to determine the thermal and dynamical impact of Sardinia on Corsican rainfall. Up to now, there exist only few studies about the influence of neighboring islands on convection initiation and most of them were made for the Maritime Continent in South-East Asia (e.g. Qian, 2008; Wu and Hsu, 2009; Wapler and Lane, 2012). In those studies, however, the island sizes were much larger than found in the Mediterranean Sea and the focus was less on local convection initiation but rather on the interactions between large-scale synoptic phenomena. The investigation of island interactions on smaller scales with respect to convective precipitation in the western Mediterranean area and the relevance of those islands for the HyMeX project in general are the main motivation for this study.

2. Method

2.1. Analyzed cases

In order to select suitable cases for our investigation, we use two criteria: (i) the existence of convective clouds on visible and infrared satellite pictures and (ii) a southerly mid-level flow. In total, six days between 2009 and 2011 are chosen for the present study (Table 1): 26 August 2009, 27 August 2009, 15 June 2010, 04 June 2011, 25 October 2011, and 05 November

Table 1

Synoptic characteristics in the Corsican area for the days under investigation and classification into two categories. The \mathbf{Q} -vector divergence is averaged in a region surrounding the Corsican island, negative values indicate convergence (upward motion), positive values indicate divergence (downward motion). The type of convection was determined by satellite observations.

Case	Position of the Corsican area	Synoptic forcing	$\nabla \cdot \mathbf{Q}$ (10^{-17} m (kg s) $^{-1}$)	Type of convection	Cat.
26 Aug 2009	Downstream of a trough	Weak	0.11	Isolated cells, heavy	(I)
27 Aug 2009	Underneath a cut-off low	Weak	1.11	Isolated cells, heavy	(I)
04 June 2011	Downstream of a cut-off low	Weak	−0.06	Isolated cells, moderate	(I)
15 June 2010	Downstream of a trough	Strong	−0.68	Embedded cells, weak	(II)
25 Oct 2011	Downstream of a trough	Strong	−0.34	Embedded cells, moderate	(II)
05 Nov 2011	Downstream of a cut-off low	Strong	−0.56	Embedded cells, moderate	(II)

2011. To characterize the synoptic situation of the selected days, we use the \mathbf{Q} -vector at 500 hPa,

$$\mathbf{Q} = -\frac{R}{p} \left(\frac{\partial \mathbf{v}_g}{\partial x} \cdot \nabla T, \frac{\partial \mathbf{v}_g}{\partial y} \cdot \nabla T \right) \quad (1)$$

where R is the gas constant of dry air, p is pressure, \mathbf{v}_g is the geostrophic wind and T is temperature. The traditional form of the quasi-geostrophic omega equation can be rewritten using the \mathbf{Q} -vector (Hoskins et al., 1978), where areas with forcing for upward (downward) vertical motion are associated with \mathbf{Q} -vector convergence (divergence). The \mathbf{Q} -vector for the simulation domain is estimated from Consortium for Small-scale MOdeling (COSMO)-EU 500 hPa analyses (Fig. 2). COSMO-EU is the operational weather forecast model of the Deutscher Wetterdienst (DWD, German Weather Service) with a horizontal grid spacing of 7 km covering the eastern Atlantic and Europe (see also Subsection 2.2). The days used for this study can be classified into two groups according to the synoptic controls: (I) weak synoptic forcing and (II) strong synoptic forcing (Table 1).

The cases of 26 August 2009, 27 August 2009, and 04 June 2011 belong to group (I), characterized by weak convergence or divergence of the \mathbf{Q} -vector (Fig. 2a, b, c). Reanalysis shows weak southerly winds in 500 hPa in the Corsican area (small gradient of geopotential) and weak synoptic-scale ascent or even descent. On the other hand, the radiosoundings of Ajaccio at the west coast of Corsica show suitable conditions for deep convection like high convective available potential energy (CAPE) of about 2000 J kg $^{-1}$ or above and small convective inhibition (CIN), except on 04 June 2011, where CAPE is moderate with a maximum of about 1200 J kg $^{-1}$ (not shown). The soundings also indicate a warm and moist low-level air ($T > 30$ °C, $T_d > 20$ °C in August 2009 and $T \approx 23$ °C, $T_d \approx 18$ °C on 04 June 2011). Firstly, satellite pictures show shallow clouds developing over Corsica and Sardinia in the morning of all cases of category (I). Immediately after midday (1100–1200 UTC), deep convective clouds form both over Corsica and Sardinia (Fig. 3a–c). The rainfall concentrates in single convective storms mainly over the land surface. The 24-h accumulated amount (0000–2359 UTC), estimated from the Tropical Rainfall Measuring Mission (TRMM) satellite data, is up to 30–40 mm both on continental Europe and islands. The TRMM weather satellite uses a microwave imager to measure precipitation amounts with a horizontal resolution of 0.25° at the surface. The data is combined with measurements of other

microwave imagers placed on other satellites to minimize systematic errors (Huffman et al., 2007).

The cases of 15 June 2010, 25 October 2011, and 05 November 2011 belong to group (II), characterized by marked convergence of the \mathbf{Q} -vector (Fig. 2d, e, f) and small or moderate values of CAPE. The synoptic situation of all three days is characterized by a deep quasi-stationary long-wave trough or cut-off over western Europe. The islands of Corsica and Sardinia are located upstream of the trough/cut-off in an area with southwesterly or southerly winds in 500 hPa and strong synoptic-scale ascent up to −40 hPa per hour or above. In all of these cases, there is cyclogenesis in the western Mediterranean. The low with an approaching cold front moves eastwards in the afternoon. In contrast to category (I), the western Mediterranean Sea has a much larger cloud cover (see Fig. 3) and precipitation occurs spatially more widespread on these days. The accumulated precipitation amount of these days (from satellite data) is up to 100–200 mm or above on a vast area along the French and Italian coasts and over the Mediterranean Sea and up to 50–60 mm over Corsica and Sardinia. On 05 November 2011, the accumulated precipitation amount is up to 200 mm over Corsica as well.

2.2. The COSMO model

The simulations were performed with the Consortium for Small-scale MOdeling (COSMO) model (Baldauf et al., 2011; Schättler et al., 2013). COSMO is a non-hydrostatic model which is used for regional weather forecasts by several European weather services including the DWD. The model employs a rotated horizontal grid (Arakawa-C) with a grid spacing of 2.8 km and 50 vertical layers in generalized terrain-following coordinates. Thus, it is capable of resolving deep convection explicitly. Shallow convection is parameterized using a modified Tiedtke scheme (Tiedtke, 1989). The surface fluxes of momentum, heat, and moisture provide for the coupling between the atmospheric part of the model with the soil and vegetation part of the model (Doms et al., 2011). We used model version 4.18.

Initial and boundary data come from hourly COSMO-EU analyses which were also used for determination of the large-scale forcing in the previous section (horizontal grid spacing of 7 km). All model runs were initialized at 0000 UTC with an integration time of 24 h. The simulation domain is the western Mediterranean between 1° and 15° eastern longitude and between 34° and 47° northern latitude (Fig. 1a) and contains an area of 545 × 595 grid points. The Corsican topography in the COSMO model is characterized by a maximum elevation of up

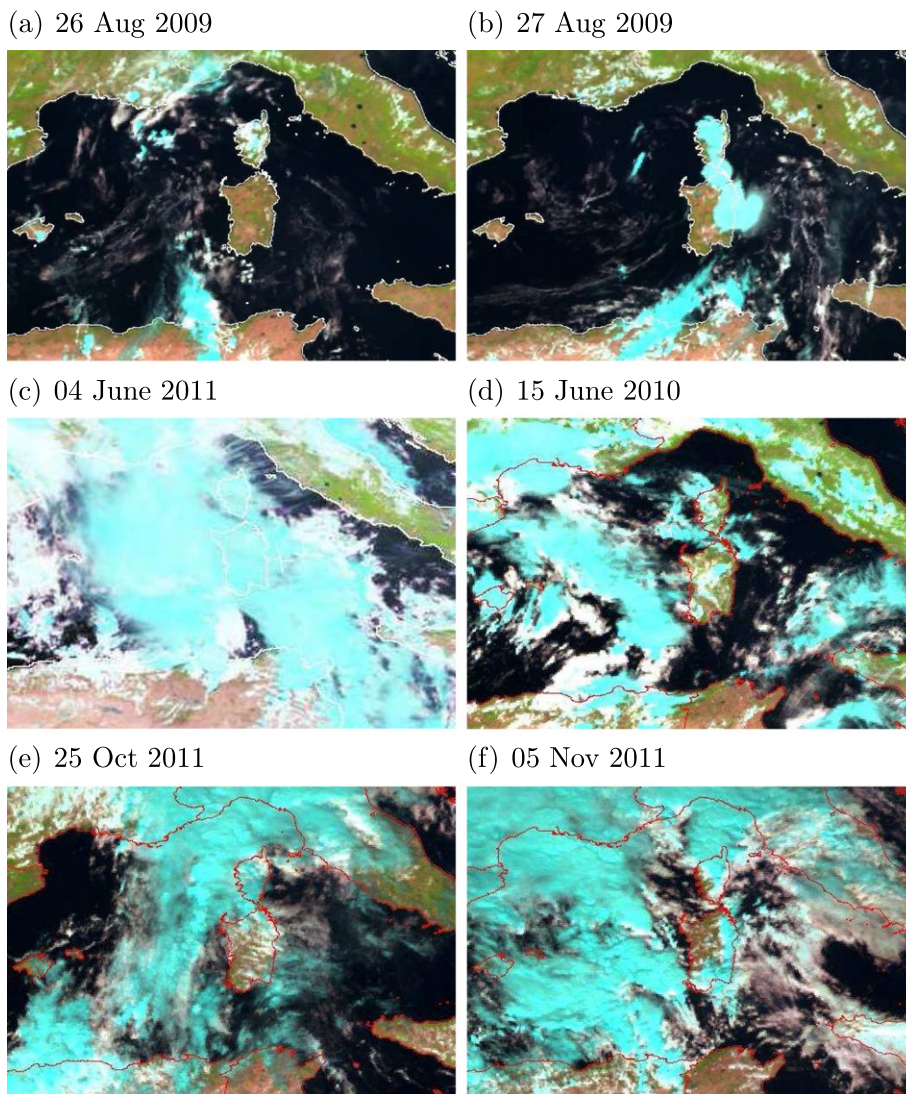


Fig. 3. Meteosat satellite pictures at 1200 UTC on days of category I (a–c) and category II (d–f). The light blue color indicates ice clouds at higher levels.

to 2000 m above mean sea level (Fig. 1b) which is notably lower than the real height of about 2700 m amsl.

First, a reference run (REF) was performed using the standard topography of the COSMO model. Then, two sensitivity runs were performed with modified topography. In one sensitivity run, Sardinia was completely removed from the external data (NOSAR) and in the other, the maximum elevation of Sardinia was restricted to 10 m (FLATSAR). In the case of a complete removal of Sardinia, each land grid point of the island was set to a sea grid point in the external data file. In the flat representation of Sardinia, only the height of the orography was modified, the other surface characteristics (soil type, land use, roughness length) remained unchanged. In both cases, the preprocessor of the COSMO model (Schättler, 2013) extrapolates all necessary fields to the new surface conditions. There is an initial phase of 2–3 h in every run in which the model adjusts to the new orographic conditions and to the initial and boundary data.

3. Results

3.1. Convective precipitation

In order to evaluate whether the reference run provides a suitable basis for our investigation and the sensitivity runs, we compare 24-h and 3-h precipitation accumulations from the reference run with data from TRMM measurements. As the horizontal resolution of the TRMM data at the surface is much lower than in our simulations, this intercomparison is conducted qualitatively only. In both categories (I) and (II), the simulated spatial distribution of precipitation agrees reasonably well with TRMM measurements (not shown). In category (I), the precipitation occurs mainly over land and on the lee side of the islands and their main mountain ranges. Although there are some differences with respect to the areas covered with rain and the 24-h accumulated precipitation, the overall agreement is

satisfactory. The same applies to the 3-h accumulations where the COSMO model simulates precipitation more or less at the same time as observed. In category (II), more noticeable differences exist. On these days, the precipitation is more influenced by large-scale processes and occurs both over land and over sea. The 24-h accumulated amount is much higher than in category (I). The regional difference between COSMO and TRMM is higher, too, especially over the Mediterranean Sea, where there is less precipitation simulated by the model. Additionally, precipitation in the model occurs around 2–3 h later than observed. Nevertheless, it can be stated that the COSMO model captures the observed convective activity in both categories reasonably well.

When comparing the 24-h accumulated precipitation over Corsica, there are pronounced differences between the three runs for individual days as well as between the two categories themselves (Fig. 4). Days of category (I) reveal lower precipitation amounts of $0.3\text{--}1.0 \cdot 10^{11}$ L than days of category (II) with values between 1.2 and $4.7 \cdot 10^{11}$ L (Fig. 4a). For example, the case of 05 November 2011 is one in a series of heavy precipitation events along the Gulf of Genoa in early November 2011 (Silvestro et al., 2012). The largest relative deviation of the accumulated precipitation of the runs NOSAR and FLATSAR from the reference run lies between -30% on 27 August 2009 and $+220\%$ on 26 August 2009 (Fig. 4b). Furthermore, there is no systematic behavior of the precipitation deviation from the reference run: In category (I), all sensitivity runs provide either increased or reduced precipitation amounts (two cases increasing, one decreasing). In

category (II), the response to the modified orography is more complex: A reduction of 24-h accumulated precipitation is simulated for all days where Sardinia is removed. When the height of Sardinia is restricted to 10 m, only a small rain reduction is simulated for 15 June 2010 (-1%) and 5 Nov 2011 (-4%) whereas a strong increase is present on 25 October 2011 ($+24\%$).

Another important point is whether the increase in precipitation is due to higher maximum precipitation amounts or larger precipitating areas (or a combination of both). As shown in Fig. 4c–d, the fraction of land points with precipitation shows more variability between individual model runs on days of category (I) than in category (II). With more large-scale forcing present on days with category (II), precipitation is simulated more spatially widespread and the response of rain coverage to terrain modifications is weak. For two cases, all island grid points are covered with precipitation in all sensitivity runs (15 June 2010 and 05 November 2011) whereas there is a small variation on 25 October 2011 with about 90% in the reference run and about 92% in the FLATSAR run. In category (I), the precipitation increase of the sensitivity runs on 26 August 2009 is a result of both a larger rain coverage and a higher maximum precipitation amount (by either more intense or longer lasting showers). The decrease on 27 August 2009 is due to a combination of smaller precipitation area and lower maximum precipitation amounts. On 04 June 2010, the precipitation increase in the NOSAR and FLATSAR runs are due to larger precipitating areas since the maximum precipitation amount is similar to the one from the REF run. The largest differences between the sensitivity runs

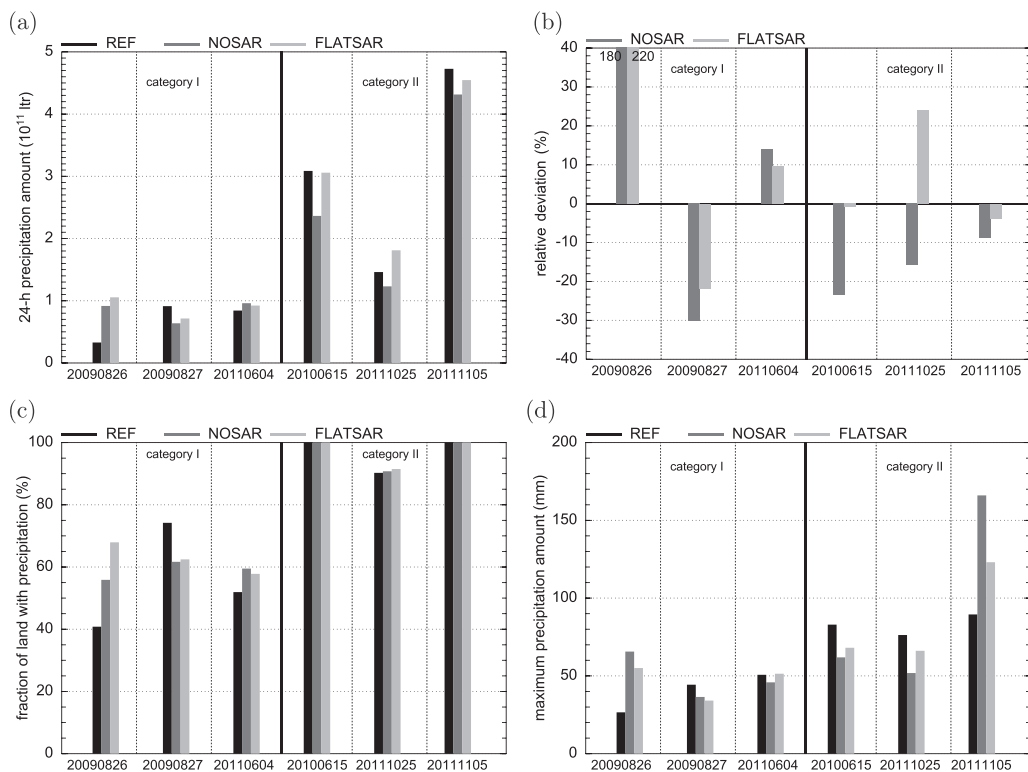


Fig. 4. 24-h accumulated precipitation (a), relative deviation of accumulated precipitation from the reference run (b), fraction of land points with precipitation (c), and maximum 24-h precipitation amount (d). REF = reference run, NOSAR = Sardinia removed, FLATSAR = maximum elevation of Sardinia restricted to 10 m amsl.

exist on 26 August 2009 where the fraction in the NOSAR run is about 15% larger and in the FLATSAR run about 28% larger than in the reference run. The maximum 24-h precipitation amount on this day in NOSAR and FLATSAR (Fig. 4d) is almost twice as much as the one from the reference run. In the case of 05 November 2011, the difference is remarkable, too, while it is small in all other cases.

The different total precipitation amounts of the sensitivity runs can also result from temporal variations. In category (I), the time evolution of precipitation is very similar on all days (see Fig. 5a for 26 August 2009 exemplarily). In the reference run, the first prominent amount of rain occurs after 1100 UTC followed by a steep increase in rain intensity until the maximum is reached at 1330 UTC. The temporal development of the FLATSAR and NOSAR runs is similar to the REF run. However, maximum rain intensities are almost twice as high as in the REF run (leading to a higher total precipitation amount) and the maximum occurs 0.5–1 h later. On 27 August 2009 (not shown), the reference run simulates a secondary precipitation maximum in the afternoon with almost the same intensity as the maximum around noon. This secondary maximum is missing in the runs with modified Sardinian orography. Only in the REF run, the cold outflow of a convective system initiated over northern Sardinia leads to strong low-level convergence over southern Corsica, subsequently initiating convective rain in that area. The missing secondary maximum causes the negative deviation of the runs NOSAR and FLATSAR on that day since the maximum rain intensity and temporal evolution are similar. In category (II), the precipitation is also influenced by large-scale processes and/or frontal systems. Thus, its temporal development is more complex. The example for 05 November 2011 (Fig. 5b) reveals simulated precipitation throughout the entire 24-h period with two maxima in the early morning (0330–0530 UTC) and in the evening (2000–2100 UTC). The evening maximum is related to the passage of a cold front. More details about this event will be given later on in Subsection 3.2.2.

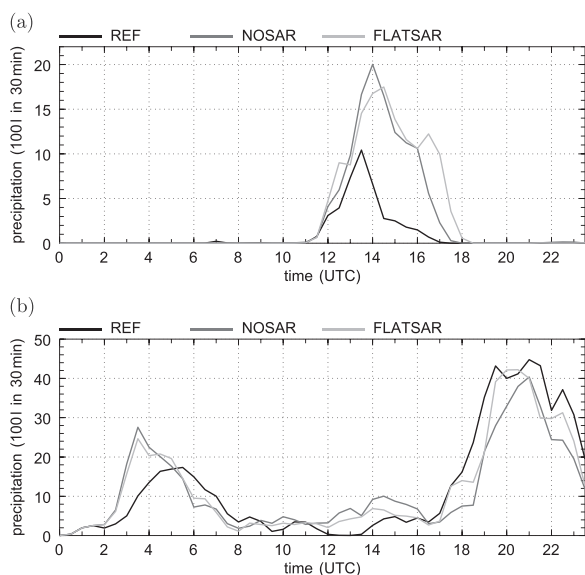


Fig. 5. Domain-averaged 30 min precipitation amount on 26 August 2009 (a) and 05 November 2011 (b).

The location of 24-h accumulated precipitation for all runs is given in Fig. 6. On all days of category (I), precipitation occurs on the lee side (with respect to the mid-tropospheric flow) of the Corsican main mountain ridge only (Fig. 6a–i). Those areas are almost identical in all sensitivity runs. When the island of Sardinia is removed, there is considerably less precipitation over Sardinia when compared to the REF- and FLATSAR runs. This indicates that the presence of a flat island is sufficient to initiate deep convection on these days. Again, the role of Sardinia is more complex on days with strong synoptic controls. The spatial distribution in category (II) reveals precipitation both over land and sea with very similar structure (Fig. 6j–r). However, the maximum values do change in the sensitivity runs, e.g. the maximum precipitation amount on 05 November 2011 in the North of Corsica is increased in the NOSAR- and FLATSAR runs when compared to the REF run. In summary, differences arise both from spatial distribution and intensity in category (I), while in category (II) they mostly occur due to varying intensity.

3.2. Convection-initiating mechanisms

To explain the differences in the precipitation amount described in the previous section, we now analyze mean and spatially integrated convection-relevant parameters for the land points of Corsica. A thorough discussion of all six days would be exhaustive, therefore we focus on one case of each category. For category (I), we choose 26 August 2009. In this case, the accumulated precipitation in the sensitivity runs differs the most. 05 November 2011 is chosen for category (II) because of the highest accumulated precipitation. Additionally, there have been some heavy precipitation events in the Gulf of Genoa in early November 2011 (including this case).

3.2.1. Category (I): 26 August 2009

The presence of Sardinia to the south of Corsica has a distinct influence on the low-level wind field and, as a consequence, also on near-surface meteorological variables. While the south-westerly flow at 700 hPa is merely identical in all simulations (not shown), remarkable differences at lower levels exist (Fig. 7). To avoid the influence of convective rain, we analyze pre-convective conditions at 1030 UTC. In the reference run, the presence of both mountainous islands leads to a channeling of the flow in an easterly direction between Corsica and Sardinia (i.e. the Strait of Bonifacio). A portion of the flow turns northward, while the remainder turns southward. Both parts then reach the respective islands and foster the sea breeze at the respective coast. The channeling of the flow is also simulated in the FLATSAR run, but with lower intensity. An important point is the fact that this easterly flow is turning towards the islands already slightly westward of the shortest island separation in the Strait of Bonifacio, whereas in the reference run, it occurs more in the lee of the islands. This has important implications for the meteorological variables over the island since now there is a sea breeze along the entire coast line of Corsica. When the island of Sardinia is removed, there is a rather uniform south–south-easterly low-level flow which brings maritime air over Corsica's southern coast. A common feature of both sensitivity runs is an increased wind speed (about +30% from the REF run) along the entire east coast strengthening the local sea breezes. For mountainous islands

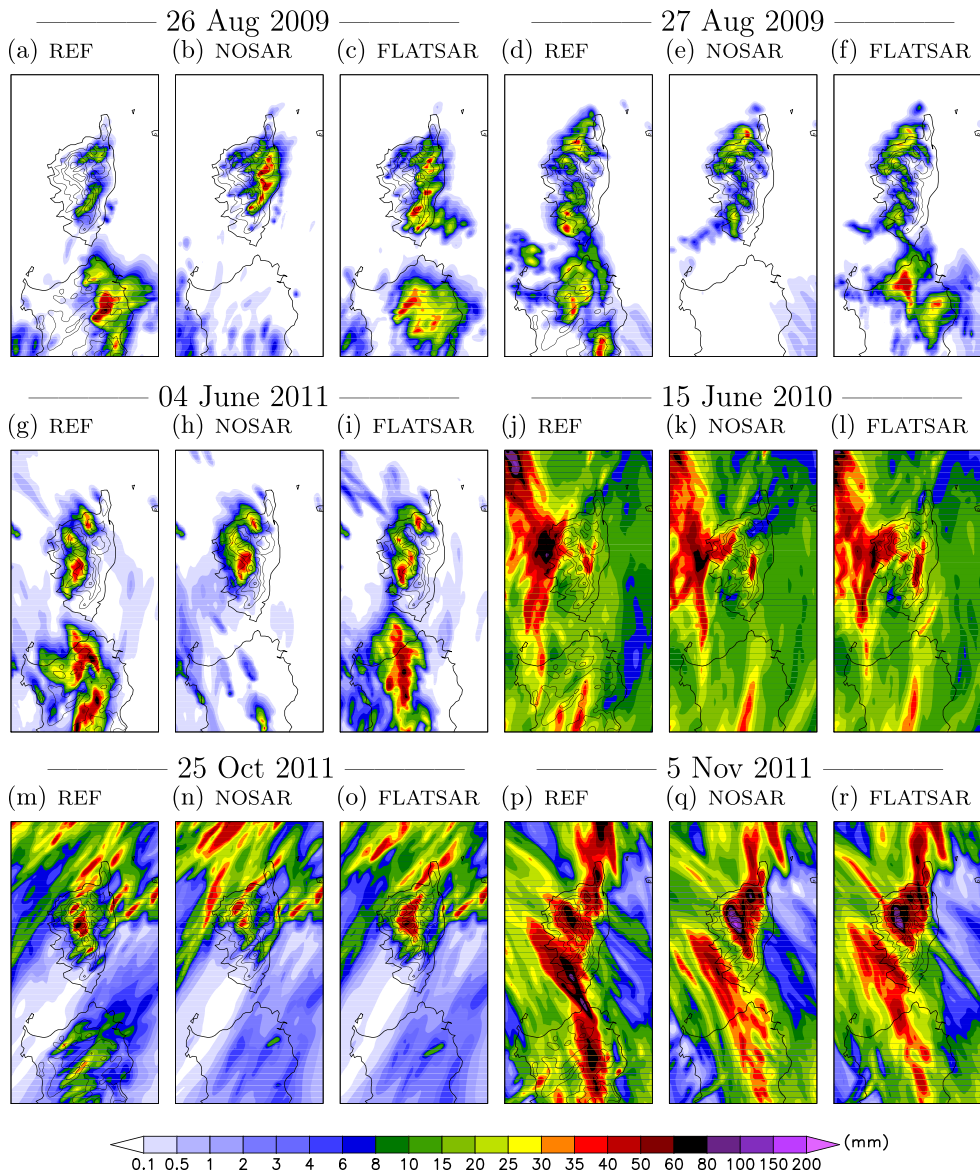


Fig. 6. 24-h accumulated precipitation on 26 August 2009 (a–c), 27 August 2009 (d–f), 04 June 2011 (g–i), 15 June 2010 (j–l), 25 October 2011 (m–o) and 05 November 2011 (p–r).

like Corsica, an interaction of the sea breeze with up-valley winds is typical (e.g. Barthlott and Kirshbaum, 2013). A strengthened sea breeze is supposed to foster up-valley winds, too. In the case of 26 August 2009 as well as in other cases of category (I), there are sea breezes and up-valley winds on both the west and east coasts. As a result, there is a convergence zone over the main mountain ridge (Fig. 7). Moreover, the missing channeling enables the development of a sea breeze and corresponding up-valley winds along the southern coast of Corsica as well. Together with the winds from the west and the east, it intensifies the convergence over the mountains. Along with the southwesterly mid-tropospheric flow, precipitation occurs somewhat downstream of the convergence zone located over the main mountain ridge.

To examine the strength of low-level convergence in our simulations, the divergence of the 10 m wind field was calculated, and only the convergent contributions were accumulated from the island land points (Fig. 8a). It can be seen that both sensitivity runs with modified topography reveal slightly higher values than in the reference run between 1000 and 1200 UTC (Fig. 8a). After 1200 UTC, the domain-averaged rain intensities in these runs are also higher than in the REF run (see Fig. 5a). A number of previous studies emphasized the role of lifting by low-level convergence for the initiation of convection (e.g. Raymond and Wilkening, 1982; Wilson and Schreiber, 1986; Kalthoff et al., 2009; Barthlott et al., 2011). Besides a low-level trigger mechanism given by this convergence, other convection-related parameters must

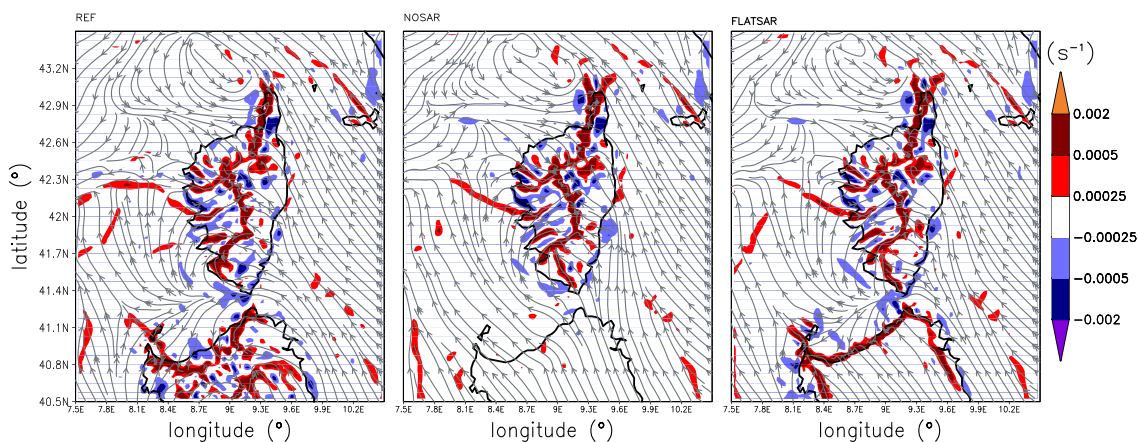


Fig. 7. 10 m horizontal wind field (streamlines) and convergence (colors) of the REF run (left), the NOSAR run (middle) and the FLATSAR run (right) on 26 August 2009 at 1030 UTC.

be favorable to allow for the development of deep moist convection.

With weak large-scale pressure gradients and solar insolation in the morning hours, thermally induced wind systems like sea breeze and upslope winds occur in the planetary boundary layer (PBL). Between 0900 and 1300 UTC, the sensitivity runs show a slightly increased total cloud cover compared to the one simulated by the reference run (Fig. 8c). In the latter, the decreased cloud coverage is caused almost entirely by a decrease of low and mid-level clouds (not shown). As a consequence, the radiation balance and the sensible heat flux are increased while the latent heat flux is slightly reduced (not shown). Despite the smaller insolation, the 2 m equivalent potential temperature θ_e is larger in both sensitivity runs when compared to the reference run. Therefore, it is mainly influenced by advective processes which are related to the flow characteristics. As a consequence of the missing or weakened channeling between Corsica and Sardinia in NOSAR and FLATSAR, the temperature and humidity along South-East Corsica are more affected by advection than in the REF run. In contrast, at the southwesterly coast, the wind additionally blows from sea to land which reduces the temperature in that area. In both areas, the coastal specific humidity increases but the weakened winds in southern Corsica slow down its inland transport also. Nevertheless, there is a transport of specific humidity by the enhanced sea breezes at the western and eastern coasts. As obvious from Fig. 8b, the FLATSAR and NOSAR runs reveal larger maximum values of θ_e than the REF run. As for the low-level convergence, the values of the sensitivity runs are increased compared to the REF run after 1000 UTC. The time series of domain-averaged CAPE follows the temporal development of θ_e since CAPE directly depends on low-level humidity and temperature (Kohler et al., 2010). In the time frame when CAPE is increased, CIN is reduced accordingly and the atmospheric conditions for deep convection improve (Fig. 8e). The domain-averaged CAPE is up to 2400 J kg^{-1} with the highest values shortly before rainfall starts (Fig. 8d). Simultaneously, CIN decreases with a domain-averaged minimum of about 10 J kg^{-1} (Fig. 8e).

In order to release CAPE, either CIN has to vanish (e.g. when the near-surface temperature reaches the convective temperature) or CIN must be overcome by rising air parcels. This rising

can either be due to low-level convergence or orographic lifting and needs to be higher than $w_{\text{CIN}} = \sqrt{2 \cdot \text{CIN}}$ (Trier, 2003). With the maximum vertical wind below the level of free convection (LFC) w_{max} , we calculate

$$w_{\text{diff}} = w_{\text{max}} - w_{\text{CIN}}. \quad (2)$$

Positive values indicate sufficient strong vertical winds to overcome CIN with subsequent release of CAPE (Adler et al., 2011). Deep convection may then develop if the entrainment of drier environmental air in the middle troposphere is not too strong. As described above, there is a remarkable convergence zone along the Corsican main mountain ridge. In this area, the vertical velocity below the LFC attains the highest values (not shown). The number of grid points where w_{diff} is positive and CAPE is higher than 2000 J kg^{-1} is displayed in Fig. 8f. After around 0800 UTC, a strong increase of this number of grid points is simulated by all model runs. This increase is clearly linked to the higher values of low-level convergence and CAPE. After 0930 UTC, both sensitivity runs now reveal more grid points fulfilling these criteria than the reference run. The highest rain intensity is simulated by the NOSAR run which also has the highest number of grid points with positive w_{diff} . As a result of increased CAPE and low-level convergence together with the reduced CIN, the number of grid points with positive w_{diff} values is up to 30% higher in FLATSAR run and up to 50% higher in NOSAR run. The maximum numbers are reached shortly after the onset of the convective precipitation (see Fig. 5a). Another noticeable difference between the REF run and the sensitivity runs displayed in Fig. 8 exists between 1500 UTC and 2000 UTC. Due to the lower rain intensities of the REF run, the low-level θ_e and CAPE are higher and CIN is lower than in both sensitivity runs.

Although the main focus of this paper lies on the Corsican rainfall, it is also interesting to analyze the orographic influence on convection over Sardinia on that day. Therefore, only the reference run and the run with restricted maximum elevation are considered since there is no deep convection in that area when Sardinia is removed. In the FLATSAR run, a north–south-oriented convergence zone is simulated in the center of the island at 1400 UTC (Fig. 9a). This convergence zone is the result of a sea breeze front which was simulated at 1000 UTC over the

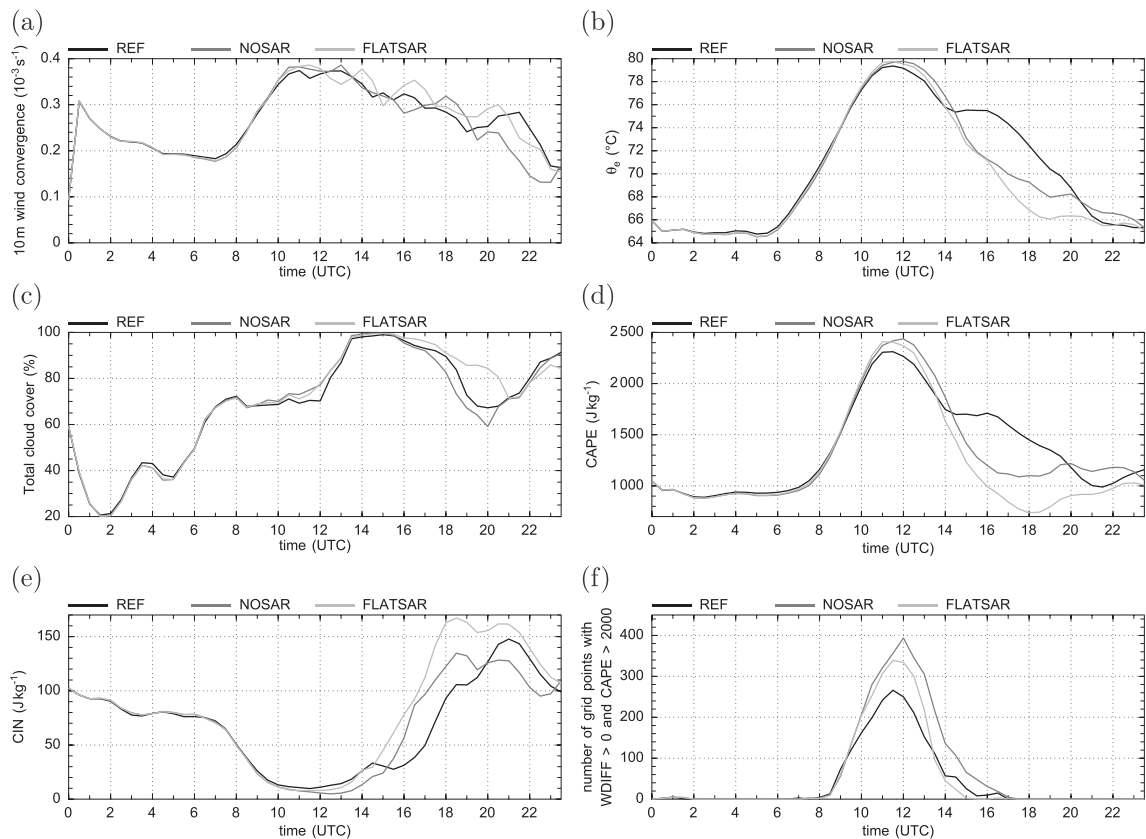


Fig. 8. Domain-accumulated 10 m wind convergence (a), domain-averaged 2 m equivalent potential temperature (b), total cloud cover (c), convective available potential energy (d), convective inhibition (e), and number of grid points with $w_{diff} > 0 \text{ m s}^{-1}$ and $CAPE > 2000 \text{ J kg}^{-1}$ (f) on 26 August 2009.

entire west coast and subsequently toward the island interior. The central alignment of the north–south-oriented convergence zone in that run is mainly a result of the missing mountains and more or less similar wind speeds on both sides. With daytime heating and the moisture supply from both sides, this convergence zone leads to the development of deep convection along the northern part of the convergence zone (Fig. 9b). A convergence zone is also simulated in the reference run with standard model orography (Fig. 9c). However, it is less organized than in the FLATSAR run because of the interaction with the orographic features and the superposition of the sea breeze with upslope winds. The main convergence zone lies more in the east of the island which leads to precipitation along the northeastern part (Fig. 9d). The total 24-h rain amount in a box surrounding Sardinia is rather similar in both runs (FLAT = $2.55 \cdot 10^{11} \text{ L}$; REF = $2.51 \cdot 10^{11} \text{ L}$). However, when integrating over the island land points only, the FLAT run reveals a higher rain amount ($2.0 \cdot 10^{11} \text{ L}$) than the REF run ($1.68 \cdot 10^{11} \text{ L}$). This reflects the more central location of the convection in that run when compared to the reference run whose precipitation falls closer to the sea.

3.2.2. Category (II): 05 November 2011

On that day, there is a strong southerly flow at 500 hPa turning to a south-easterly direction during the day (see Fig. 2). The near-surface flow on that day is strong, too, with south-easterly winds of about 13 m s^{-1} over the open sea and partly

over land as well (not shown). Due to the more southerly wind direction, there is no channeling between Corsica and Sardinia. In addition, the strong synoptic-scale flow and the greater cloud coverage inhibit the buildup of thermally induced land–sea breeze circulations or mountain–valley winds. The synoptic flow conditions rather induce permanent sea breezes and up-valley winds on the eastern side of Corsica and land breezes or down-valley winds on the western side. The sole exception is the very North-West. The strong flow around Corsica induces a wake and therefore a sea breeze at the northwestern coast (not shown). In contrast to the example for category (I), this day is not characterized by daytime convection as a response to solar heating of the land. Moreover, all model runs simulate precipitation for almost the entire day as evident from Fig. 5b. The maximum rain intensities occur in the evening due to the passage of a cold front.

Since the upstream flow is less affected by the orography in the NOSAR and FLATSAR runs, the inflow velocity in the south and southeast of Corsica is increased. As a result of that, the low-level convergence in that area is higher while it is nearly of equal size over the rest of Corsica. This increase is the main reason for the higher accumulated low-level convergence in the NOSAR and FLATSAR runs present almost the entire day (Fig. 10a). Between 0200 and 0600 UTC, the convergence increase of the sensitivity runs matches that of the higher rain intensities when compared to the reference run. During that time, due to the missing solar radiation, the increase of θ_e in the

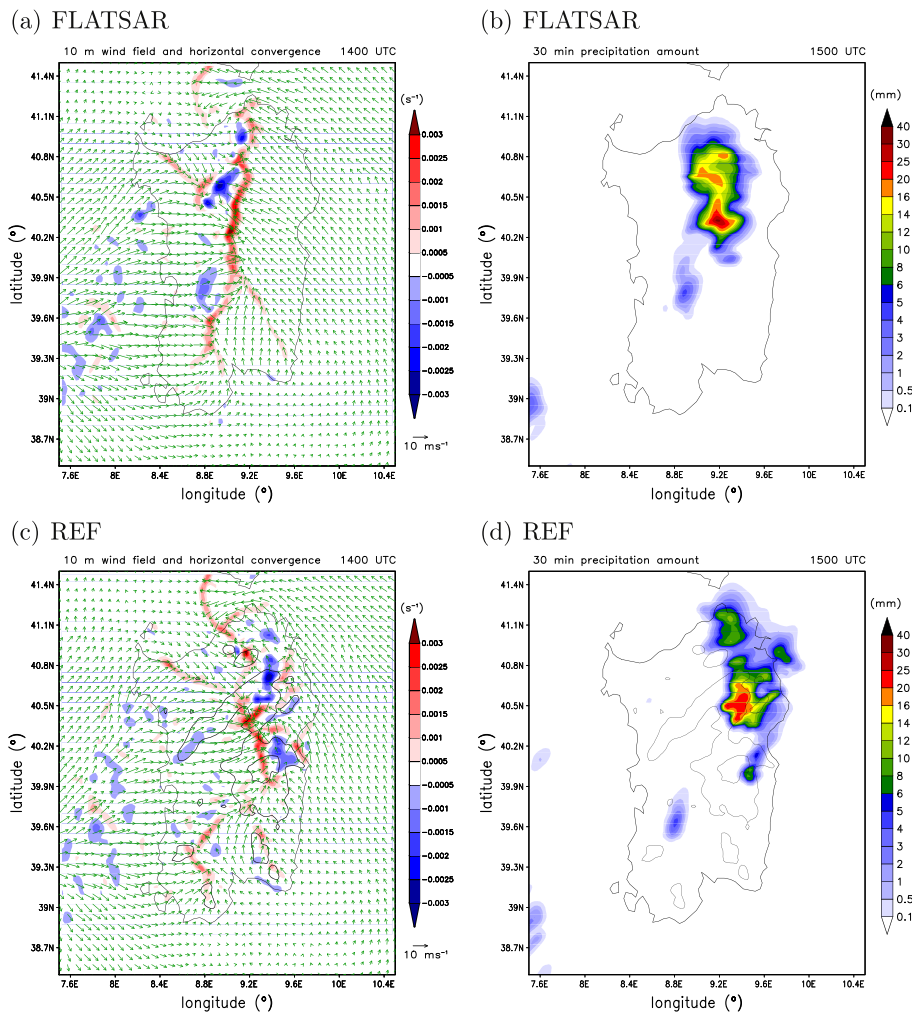


Fig. 9. 10 m wind convergence at 1400 UTC (a, c) and 30-min precipitation amount at 1500 UTC (b, d) on 26 August 2009.

runs NOSAR and FLATSAR is a result of advective processes related to the different flow conditions (Fig. 10b). Whereas CAPE is almost identical in all model runs, the domain-averaged CIN is about 15 J kg^{-1} smaller in both sensitivity runs. The nocturnal maximum rain intensity of the reference run is at 0530 UTC whereas both sensitivity runs reach their maximum 2 h earlier (see Fig. 5). The reduction of convective inhibition in the sensitivity runs is simulated almost the entire day until the thermodynamical conditions are influenced by the approaching cold front after 1800 UTC.

Between 0600 and 1000 UTC, the sensitivity runs also simulate higher values of low-level θ_e as the reference run. This increase is mainly attributed to a strong increase of specific humidity, whereas the temperature increase is small only (not shown). As a consequence, the averaged CAPE is about 20% higher in the sensitivity runs (Fig. 10d) but with values of about 600 J kg^{-1} remarkably lower than in category (I). The domain-averaged CIN (Fig. 10e) in the reference run is about 50% higher than in the sensitivity runs ($10\text{--}20 \text{ J kg}^{-1}$ around noon). Although in both sensitivity runs, the conditions for convective precipitation do improve (higher CAPE, lower CIN,

more grid points with positive w_{diff}), these runs do simulate less precipitation than the reference run. A possible explanation for that might be the fact that on this day, the large-scale forcing plays a greater role and that precipitation is only partly controlled by surface and boundary-layer processes.

Later in the day, the cloud cover decreases to values of about 80–87% between 1300 and 1500 UTC (Fig. 10c). This decrease is due to the total dispersal of high-level clouds (not shown). Ahead of the mid-level low analyzed in Subsection 2.1, there is a potential vorticity-anomaly passing over Corsica and Sardinia around midday. A marked decline of the specific humidity in high altitudes indicates the possible intrusion of dry stratospheric air which could have led to the dispersal of high-level clouds. There is no such signal in the domain-average of mid- and low-altitude clouds.

From 1800 UTC on, a cold front reaches Corsica from the south-west. In terms of precipitation amount, it is the dominating event on that day because the highest 30 min precipitation rates (more than $40 \times 10^2 \text{ L } 30 \text{ min}^{-1}$) and most of the daily precipitation occur during the time of the front passage. Although the maximum precipitation rates are rather similar in

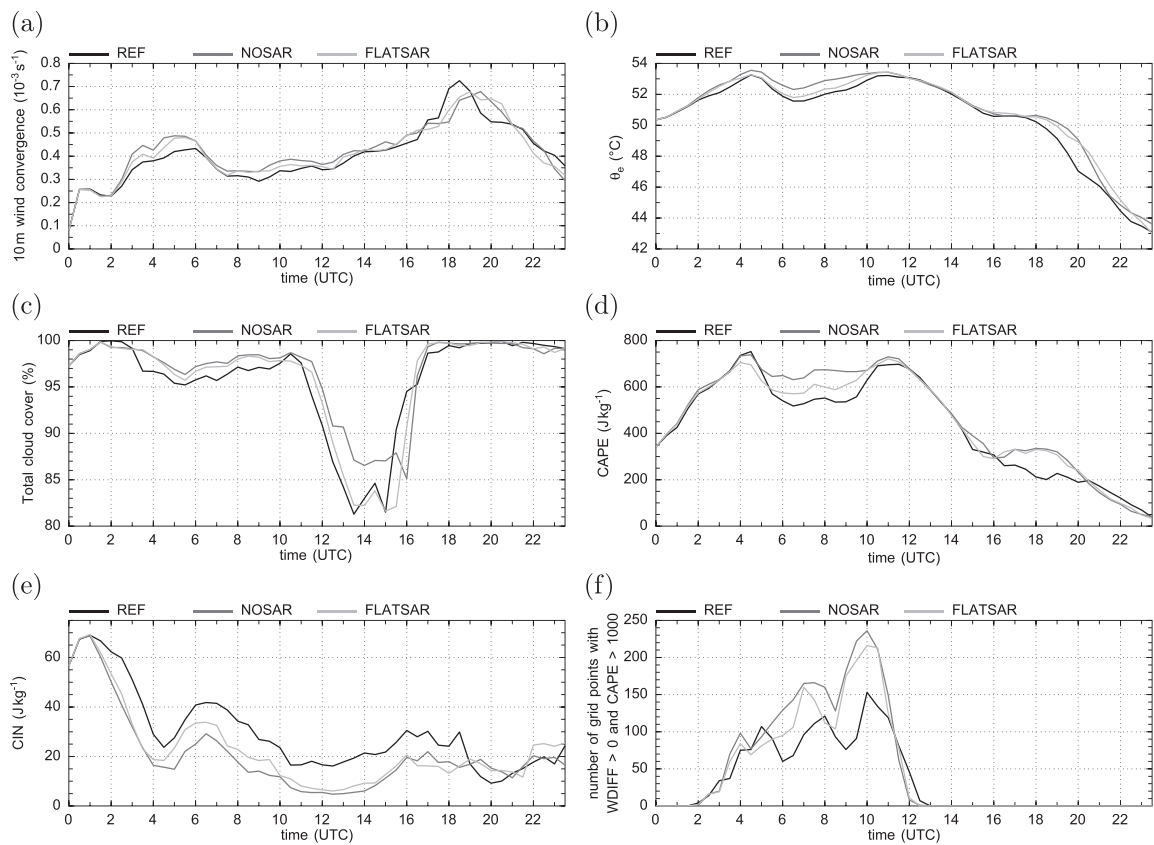


Fig. 10. Domain-accumulated 10 m wind convergence (a), domain-averaged 2 m equivalent potential temperature (b), total cloud cover (c), convective available potential energy (d), convective inhibition (e), and number of grid points with $w_{diff} > 0 \text{ m s}^{-1}$ and $CAPE > 1000 \text{ J kg}^{-1}$ (f) on 05 November 2011.

all model runs (Fig. 5b), the time period with a spatially integrated precipitation rate of more than $20 \times 10^2 \text{ L } 30 \text{ min}^{-1}$ is about 1.5 h longer in the reference run. During the passage of the front, several meteorological variables show significant changes: due to the stronger rain intensities, CAPE is reduced in the reference run particularly between 1600 and 2000 UTC. There is a cyclonic shift of almost 90° in the near-surface wind direction with a south-easterly prefrontal and a south-westerly post-frontal flow with the wind speed slowing down from $13\text{--}15 \text{ m s}^{-1}$ to $2\text{--}4 \text{ m s}^{-1}$. Furthermore, the 2 m temperature and specific humidity decrease about 5 K and $4\text{--}5 \text{ g kg}^{-1}$, respectively (not shown). In general, this applies to all three implemented simulations, but there are distinct differences in location, orientation, and translation speed of the front itself with an impact on the strength and spatial distribution of low-level convergence and precipitation triggering. The cold front is oriented from northwest to southeast. On its way through the Mediterranean Sea towards the northeast, it first reaches the island of Sardinia. In the reference run, the front slows down in that area while more northward, it speeds up. The northern part therefore arrives at the southwest of Corsica about 0.5 h earlier than in the NOSAR or FLATSAR run (Fig. 11). Additionally, the accelerated winds then yield to a stronger low-level convergence over southern Corsica in the reference run, the domain-average is about 20% higher than in the sensitivity runs. During its passage over Corsica, the corresponding part of the front slows down again and the northern and southern parts accelerate. This

time, there is an angular modification, too. Over Corsica, the front has the same north-to-south extent as the main mountain ridge, whereas it first maintains its original orientation over the sea. After the front has passed Corsica, its orientation is still from northwest to southeast in the reference run, but it has changed to a more east-southeast to west-northwest alignment in NOSAR and FLATSAR runs. Altogether, the passage lasts longer in the reference run and causes stronger low-level convergence. Therefore, we conclude that the increased low-level convergence is responsible for the stronger rain intensities and increased precipitation amount in the reference run.

4. Discussion and conclusions

The numerical simulations presented herein investigate the role of Sardinia on Corsican rainfall in the western Mediterranean Sea. Whereas the island of Corsica is left intact in all simulations, sensitivity runs were performed in which Sardinia was either completely removed or its maximum elevation restricted to 10 m. The analyses of six cases with either weak (category I) or strong (category II) synoptic forcing revealed a complex relationship between these neighboring islands. The simulated 24-h precipitation amounts were generally larger on days of category (II) in which, with the exception of one single model run, all simulations with modified Sardinian topography lead to a reduced precipitation amount when compared to the reference run. The most pronounced precipitation deviation

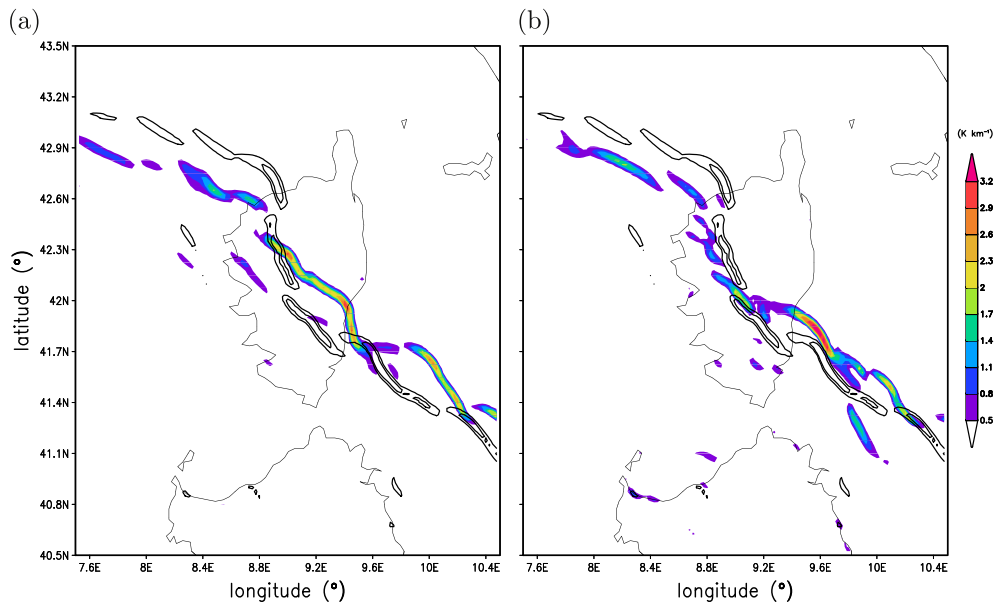


Fig. 11. Horizontal west–east gradient of 2 m equivalent potential temperature (colors) at 2100 UTC on 05 November 2011 for the NOSAR run (a) and the FLATSAR run (b). The thick black contours indicate the 0.8 K km^{-1} and 2.0 K km^{-1} isolines of the reference run.

from the reference run (i.e. an increase of 220%) occurred on a day with prevailing weak synoptic forcing. In this category, the precipitation deviation was either positive or negative in the sensitivity runs of the respective day, but without a systematic dependance on the Sardinian orography. While precipitation differences in category (I) arose both from slightly different spatial distributions and intensity of convective rain, they mostly occurred due to varying intensity in category (II).

The proximity of Corsica to a second island which is not as high in elevation, but roughly three times as big in horizontal extent, has important effects on the low-level wind field as well as the temperature and moisture distribution. The most pronounced difference in the low-level flow structure occurred in the runs in which the island of Sardinia was removed. As there is no blocking or flow deviation of the southerly flow, maritime air can now be transported also over Corsica's southern coast. Together with the strengthened wind speeds in that area, Corsica then possesses a higher moisture content with increased values of low-level convergence. Thus, the conditions for the development of deep convection improve due to stronger low-level ascent and more favorable convective indices.

The channeling of the flow between both islands is simulated in the reference run and, in an attenuated form, also in the run with a flat representation of Sardinia. In the latter, the flow turns northward towards Corsica already shortly after the passage of the Strait of Bonifacio, which also increased the advection of moist air towards Corsica. The increased precipitation amount could be attributed to changes of low-level convergence and moisture/heat content and their effect on thermodynamic parameters, like convective available potential energy or convective inhibition.

Besides the aforementioned direct effects related to the different representations of Sardinia's orography, the convective processes initiated over Sardinia can also have a large impact on

Corsica. In one case, a cold pool of a convective system over northern Sardinia leads to an almost circular shaped outflow region with increased low-level winds and strong convergence at the leading edge. The secondary triggering of convection over southern Corsica related to the lifting along this convergence zone also leads to an increased total precipitation amount. The relationship between Corsican precipitation and Sardinia was more subtle on days with strong synoptic forcing. On these days, the average percentage deviation of daily precipitation from the reference run was less than on days with weak synoptic forcing. This indicates the smaller role of the topography in those cases and that rainfall is only partly controlled by boundary-layer processes related to the topography. However, the presence of Sardinia had a strong influence on the position and translation speed of a cold front. In one case, the reduced precipitation amounts from a frontal passage of a few hours only lead to a reduction of total precipitation, despite the larger rain intensities throughout most of the rest of the day.

Even if the six case studies analyzed herein are not sufficient for general statements (as obvious from the different precipitation modifications in our simulations with respect to Sardinia's orography), the results indicate the high impact of the proximity of Sardinia to the Corsican rainfall. The modification of the flow field by Sardinia's topography and the triggering of convective cells over Sardinia have important implications for the thermodynamic and kinematic conditions over Corsica. To conclude, these results demonstrate that an adequate representation of detailed topographic features is necessary to correctly describe the interaction processes between these islands.

Acknowledgments

This work is a contribution to the HyMeX program. The authors wish to thank the Deutscher Wetterdienst (DWD) for providing the COSMO model code as well as initial and

boundary data. Satellite pictures were kindly provided by F. Olesen (IMK-ASF, KIT). The TRMM data used in this study were acquired using the GES-DISC Interactive Online Visualization ANd aNalysis Infrastructure (Giovanni) as part of NASA's Goddard Earth Sciences (GES) Data and Information Services Center (DISC). The authors acknowledge Météo-France for supplying the radiosonde data and the HyMeX database teams (ESPRI/IPSL and SEDOO/Observatoire Midi-Pyrénées) for their help in accessing the data.

References

- Adler, B., Kalthoff, N., Gantner, L., 2011. Initiation of deep convection caused by land-surface inhomogeneities in West Africa: a modelled case study. *Meteorol. Atmos. Phys.* 112, 15–27.
- Baldauf, M., Seifert, A., Förstner, J., Majewski, D., Raschendorfer, M., 2011. Operational convective-scale numerical weather prediction with the COSMO model: description and sensitivities. *Mon. Weather Rev.* 139, 3887–3905.
- Barthlott, C., Kalthoff, N., 2011. A numerical sensitivity study on the impact of soil moisture on convection-related parameters and convective precipitation over complex terrain. *J. Atmos. Sci.* 68, 2971–2987.
- Barthlott, C., Kirshbaum, D., 2013. Sensitivity of deep convection to terrain forcing over Mediterranean islands. *Q. J. R. Meteorol. Soc.* 139, 1762–1779.
- Barthlott, C., Burton, R., Kirshbaum, D., Hanley, K., Richard, E., Chaboureaud, J.-P., Trentmann, J., Kern, B., Bauer, H.-S., Schwitala, T., Keil, C., Seity, Y., Gadian, A., Blyth, A., Mobbs, S., Flamant, C., Handwerker, J., 2011. Initiation of deep convection at marginal instability in an ensemble of mesoscale models: a case-study from COPS. *Q. J. R. Meteorol. Soc.* 137 (S1), 118–136.
- Bresson, E., Ducrocq, V., Nuissier, O., Ricard, D., de Saint-Aubin, C., 2012. Idealized numerical simulations of quasi-stationary convective systems over the Northwestern Mediterranean complex terrain. *Q. J. R. Meteorol. Soc.* 138, 1751–1763.
- Doms, G., Förstner, J., Heise, E., Herzog, H.-J., Raschendorfer, M., Reinhardt, T., Ritter, B., Schrodin, R., Schulz, J.-P., Vogel, G., 2011. A description of the non-hydrostatic regional COSMO-model, part II: physical parameterization Available online at <http://www.cosmo-model.org> (last access: 10.03.2014).
- Drobinski, P., Ducrocq, V., Alpert, P., Anagnostou, E., Béranger, K., Borga, M., Braud, I., Chanzy, A., Davolio, S., Delrieu, G., Estournel, C., Filali Boubrahmi, N., Font, J., Grubisic, V., Gualdi, S., Homar, V., Ivancan-Picek, B., Kottmeier, C., Kotroni, V., Lagouvardos, K., Lionello, P., Llasat, M., Ludwig, W., Lutoff, C., Mariotti, A., Richard, E., Romero, R., Rotunno, R., Roussot, O., Ruin, I., Somot, S., Taupier-Letage, I., Tintore, J., Uijlenhoet, R., Wernli, H., 2014. HyMeX, a 10-year multidisciplinary program on the Mediterranean water cycle. *Bull. Am. Meteorol. Soc.* 95, 1063–1082.
- Ducrocq, V., Nuissier, O., Ricard, D., Lebeaupin, C., Anquetin, S., 2008. A numerical study of three catastrophic precipitating events over southern France. II: mesoscale triggering and stationarity factors. *Q. J. R. Meteorol. Soc.* 134, 131–145.
- Ducrocq, V., Braud, I., Davolio, S., Ferretti, R., Flamant, C., Jansa, A., Kalthoff, N., Richard, E., Taupier-Letage, I., Ayrat, P.-A., Belamari, S., Berne, A., Borga, M., Boudevillain, B., Bock, O., Boichard, J.-L., Bouin, M.-N., Bousquet, O., Bouvier, C., Chiggiato, J., Cimini, D., Corsmeier, U., Coppola, L., Cocquerez, P., Defer, E., Delanoë, J., Girolamo, P.D., Doerenbecher, A., Drobinski, P., Dufournet, Y., Fourrié, N., Gourley, J.J., Labatut, L., Lambert, D., Le Coz, J., Marzano, F.S., Molinié, G., Montani, A., Nord, G., Nuret, M., Ramage, K., Rison, B., Roussot, O., Said, F., Schwarzenboeck, A., Testor, P., Baelen, J.V., Vincendon, B., Aran, M., Tamayo, J., 2014. HyMeX-SOP1, the field campaign dedicated to heavy precipitation and flash flooding in the northwestern Mediterranean. *Bull. Am. Meteorol. Soc.* 95, 1083–1100.
- Findell, K.L., Eltahir, E.A.B., 2003. Atmospheric controls on soil moisture–boundary layer interactions. Part I: framework development. *J. Hydrometeorol.* 4, 552–569.
- Giorgetti, J.-P., Jacq, V., Jourdan, R., Palauqui, J.-P., Rivrain, J.-C., 1994. Les pluies diluviennes et les inondations des 31 octobre et 1er novembre 1993 en Corse: étude descriptive. *La Météorologie* 6, 9–30.
- Hoskins, B.J., Draghici, I., Davies, H.C., 1978. A new look at the omega-equation. *Q. J. R. Meteorol. Soc.* 104, 31–38.
- Huffman, G.J., Bolvin, D.T., Nelkin, E.J., Wolff, D.B., Adler, R.F., Gu, G., Hong, Y., Bowman, K.P., Stocker, E.F., 2007. The TRMM multisatellite precipitation analysis (TMPA): quasi-global, multiyear, combined-sensor precipitation estimates at fine scales. *J. Hydrometeorol.* 8, 38–55.
- Kalthoff, N., Adler, B., Barthlott, C., Corsmeier, U., Mobbs, S., Crewell, S., Träumner, K., Kottmeier, C., Wieser, A., Smith, V., 2009. The impact of convergence zones on the initiation of deep convection: a case study from COPS. *Atmos. Res.* 93, 680–694.
- Kohler, M., Kalthoff, N., Kottmeier, C., 2010. The impact of soil moisture modifications on CBL characteristics in West Africa: a case-study from the AMMA campaign. *Q. J. R. Meteorol. Soc.* 136 (S1), 442–455.
- Kottmeier, C., Palacio-Sese, P., Kalthoff, N., Corsmeier, U., Fiedler, F., 2000. Sea breezes and coastal jets in southeastern Spain. *Int. J. Climatol.* 20, 1791–1808.
- Lambert, D., Mallet, M., Ducrocq, V., Dulac, F., Gheusi, F., Kalthoff, N., 2011. CORSICA: a Mediterranean atmospheric and oceanographic observatory in Corsica within the framework of HyMeX and ChArMEX. *Adv. Geosci.* 26, 125–131.
- Llasat, M.C., Llasat-Botija, M., Prat, M.A., Porcú, F., Price, C., Mugnai, A., Lagouvardos, K., Kotroni, V., Katsanos, D., Michaelides, S., Yair, Y., Savvidou, K., Nicolaides, K., 2010. High-impact floods and flash floods in Mediterranean countries: the FLASH preliminary database. *Adv. Geosci.* 23, 47–55.
- Metzger, J., Barthlott, C., Kalthoff, N., 2014. Impact of upstream flow conditions on the initiation of moist convection over the island of Corsica. *Atmos. Res.* 145–146, 279–296.
- Qian, J.-H., 2008. Why precipitation is mostly concentrated over islands in the Maritime Continent. *J. Atmos. Sci.* 65, 1428–1441.
- Raymond, D.J., Wilkening, M.H., 1982. Flow and mixing in New Mexico mountain cumuli. *J. Atmos. Sci.* 39, 2211–2228.
- Robinson, F.J., Sherwood, S.C., Li, Y., 2008. Resonant response of deep convection to surface hot spots. *J. Atmos. Sci.* 65, 276–286.
- Schättler, U., 2013. A description of the nonhydrostatic regional COSMO-model, part V: preprocessing: initial and boundary data for the COSMO-model Available online at <http://www.cosmo-model.org> (last access: 10.03.2014).
- Schättler, U., Doms, G., Schraff, C., 2013. A description of the non-hydrostatic regional COSMO-model, part VII: user's guide Available online at <http://www.cosmo-model.org> (last access: 10.03.2014).
- Silvestro, F., Gabellani, S., Giannoni, F., Parodi, A., Reboria, N., Rudari, R., Siccardi, F., 2012. A hydrological analysis of the 4 November 2011 event in Genoa. *Nat. Hazards Earth Syst. Sci.* 12, 2743–2752.
- Tarolli, P., Borga, M., Morin, E., Delrieu, G., 2012. Analysis of flash flood regimes in the North-Western and South-Eastern Mediterranean regions. *Nat. Hazards Earth Syst. Sci.* 12, 1255–1265.
- Tiedtke, M., 1989. A comprehensive mass flux scheme for cumulus parameterization in large-scale models. *Mon. Weather Rev.* 117, 1779–1800.
- Trier, S.B., 2003. Convective storms – convective initiation. In: Holton, J.R., Curry, J.A., Pyle, J.A. (Eds.), *Encyclopedia of Atmospheric Sciences* vol. 2. Academic Press, London.
- Wapler, K., Lane, T.P., 2012. A case of offshore convective initiation by interacting land breezes near Darwin, Australia. *Meteorol. Atmos. Phys.* 115, 123–137.
- Wilson, J., Schreiber, W., 1986. Initiation of convective storms at radar-observed boundary-layer convergence lines. *Mon. Weather Rev.* 114, 2516–2536.
- Wilson, J.W., Carbone, R.E., Tuttle, J.D., Keenan, T.D., 2001. Tropical island convection in the absence of significant topography: part II: nowcasting storm evolution. *Mon. Weather Rev.* 129, 1637–1655.
- Wu, C.-H., Hsu, H.-H., 2009. Topographic influence on the MJO in the Maritime Continent. *J. Clim.* 22, 5433–5448.